GRADIENT FIELD GENERATION IN A UNIFORM GAPPED MAGNET

Yoshihisa Iwashita, Kyoto ICR, Uji, Kyoto, JAPAN
Yasushi Arimoto, Akira Sato, Osaka University, Osaka, JAPAN

Abstract

A novel method to generate a gradient field in a constant gapped magnet is devised with use of inter-pole made of anisotropic magnet material. This magnet can have not only constant gap but also smaller fringing field compared with a conventional one. This technique should widen the recipe to design a magnet with a complex magnetic field distribution.

INTRODUCTION

Magnets with gradient field (indexed magnets) usually have different gap distances in accordance with the field to be generated. (see Fig. 1). Taking a line integral along Γ, the magnetic flux density at gap distance g with excitation current I is given by $B = \mu_0 I / g$, when the permeability μ in the iron is large enough. This configuration has an advantage because it needs only one set of coils and one power supply. The gap distance variation, however, will break a uniformity of the effective length for such a gradient magnet. Trim coils on a flat pole magnet may generate such a gradient field, which are usually used in Cyclotron. They are not practical to modify a field distribution when a large gradient is required such as in a combined function synchrotron [1] or FFAG [2].

In order to generate a gradient field in a constant gapped magnet, a novel method with use of inter-poles is devised. This magnet has not only constant gap but also smaller fringing field compared with a conventional one.

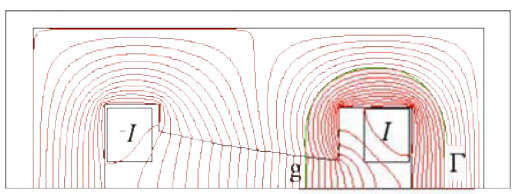

Fig. 1 A magnet with gradient field.

INTER-POLE IN A MAGNET

When we divide the pole into two sections (a flat square block and the other part) and switch the position as shown in Fig. 2, the gap distance in the vicinity of the median plane becomes constant while the total air gap length at a horizontal position does not change. Unfortunately, the bulk iron (isotropic material) surface becomes an equipotential surface; the magnetic field in the gap region becomes flat as shown in Fig. 3.

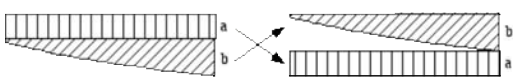

Fig. 2 Divided magnet pole parts are switched.

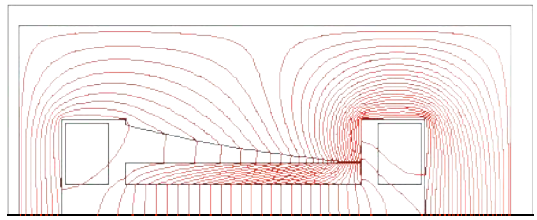

Fig. 3 A magnet with inter-pole made of bulk iron.

This situation can be cured by introducing anisotropic material as the inter-pole that has a high permeability in a direction normal to the median plane and low permeability in the direction to the field variation. Such material can be composed by a stack of high permeability iron sheets with non-magnetic spacers in between (see Fig. 4). The equivalent permeability μ_e in the stacking direction is given by

$$\mu_e = 1/(1 - p + p/\mu_n)$$

where p is the packing factor and μ_n is the permeability of the iron sheet. Usually μ_n is high enough that μ_e can be rewritten as

$$\mu_e = 1/(1 - p).$$

When the packing factor p is 0.667, the μ_e becomes only 3, while those of the other directions remain high. The resulted magnetic field distribution is shown in Fig. 5. Because the horizontal permeability is not unity, the generated field gradient becomes slightly smaller than that calculated from the sum of the length of two gaps: upper gap and median gap. Strictly speaking, the actual number of gaps in a real magnet is three, while we are considering only upper half of a magnet. There is one drawback that the low packing factor decreases the allowable magnetic flux density.

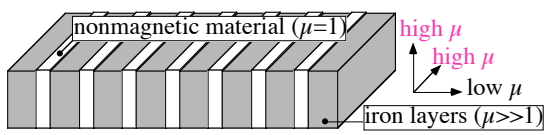

Fig. 4 Composed anisotropic material.

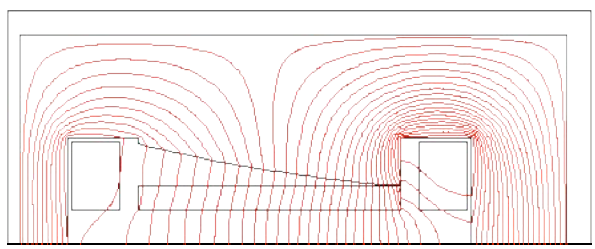

Fig. 5 Flux plot of a magnet with a set of inter-poles made of anisotropic magnet material that has low permeability (μ~3) in horizontal direction.

FRINGING FIELD UNIFORMITY

The effects of the inter-pole on the fringing field are evaluated by pole geometries with different total gap distance (see Fig. 6). The left figures show the magnets with inter-poles, while the right figures are the conventional magnets. Both cases have the same total gap distances (20cm and 40cm) to generate the same levels of magnetic field. Fig. 7 shows the field distribution, where the broken lines (G40C and G20C) show magnetic field distributions without inter-poles and the solid lines (G40 and G20) show those with inter-poles. The ratios of magnetic fields for small gap to those for large gap in both cases are also shown. When the inter-poles are used the ratio is kept fairly constant until the absolute values become less significant. The effective length was calculated by taking an integral of Bz along the horizontal axis and normalized by its maximum value. Then the effective length ratio was obtained by taking the ratio of these two values: with large gap width and with narrow gap width. The ratio for the conventional magnet was evaluated as follows:

$$\frac{\int B_z^{40C}\,ds}{B_z^{40C}@\max}\Big/\frac{\int B_z^{20C}\,ds}{B_z^{20C}@\max}=0.971,$$

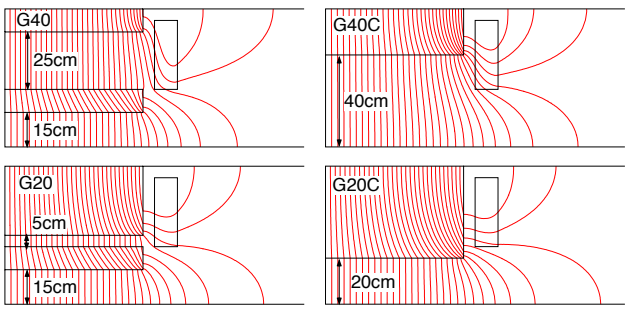

Fig. 6 Magnet configurations to evaluate the effective lengths. The left figures show the magnets with inter-poles. The right figures are the conventional magnets. The top figures represent the cross sections where the magnetic fields are weaker and the bottom ones represents the cross sections where the magnetic fields are stronger. The excitation current is 100kA.

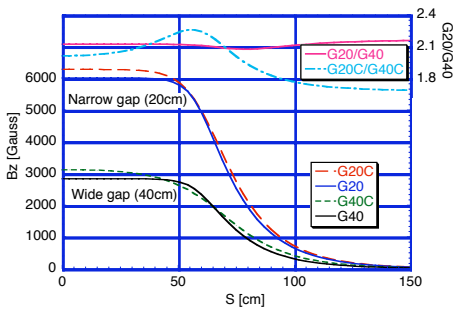

Fig. 7 The magnetic field distributions of large and small gapped magnets. When the inter-poles are used the ratio is kept fairly constant until the absolute values become less significant.

where B_z^{40C} and B_z^{20C} are the B_z components on the median planes for magnets with 40cm gap and 20cm gap, respectively. The value for the magnet with inter-pole was calculated as follows:

$$\frac{\int B_z^{40}\,ds}{B_z^{40}@\max}\Big/\frac{\int B_z^{20}\,ds}{B_z^{20}@\max}=1.003.$$

These show that the effective length can be well kept constant even with very big change in the gap distance.

POLE SHAPE AND TRIM COIL

Because the permeability of the inter-pole in the horizontal direction is slightly larger than that of vacuum, it filters out local irregularity of the magnetic field distribution. Thus the complex shaped surface may be approximated by a stepwise shape as shown in Fig. 8. This stepwise shape may be somewhat exaggerated; a moderate one may be a piecewise linear approximation. This example also has four sets of trim coils to change the field gradient. The low pass filtering function makes the locality of a trim coil less significant and the field distribution becomes smooth (see Fig. 9). This turns out to reduce the number of trim coils to achieve a field quality at a tolerance of a flutter in Bz component.

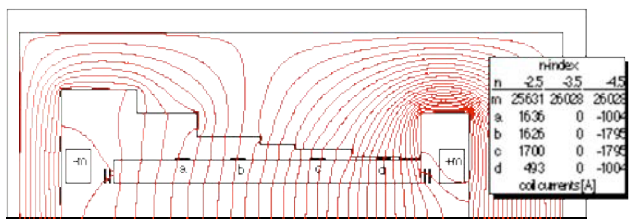

Fig. 8 A magnet with inter-pole that has stepwise approximated iron surface. This example has also trim coils to change the field index. After the step pole shape was optimized for n=-3.5 without trim coils, the positions of four coils together with the currents of the two groups are adjusted to raise the gradient to n=-4.5. Finally, all five coil currents are adjusted to decrease it to n=-2.5.

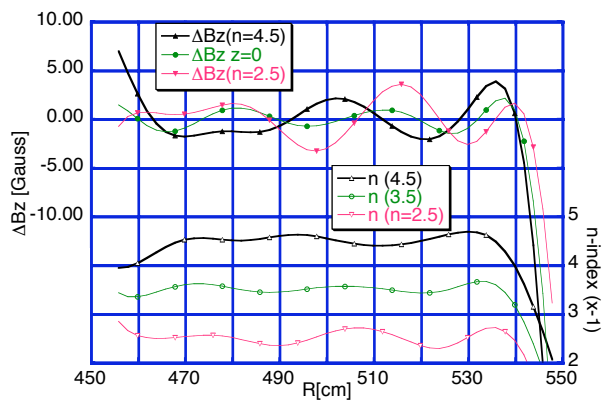

Fig. 9 Field distributions with currents on trim coils. The field index is raised to 4.5 or reduced down to 2.5 from the original value 3.5.

SINGLE EASY AXIS MATERIAL

The composed anisotropic material introduced and discussed in the above sections has high permeability in two directions. These directions can be reduced to only one by applying a configuration shown in Fig. 10 and Fig. 11: the magnetic materials are inserted in grids made of nonmagnetic separators. This kind of composed material at magnet edges can reduce an absolute value of the fringing filed.

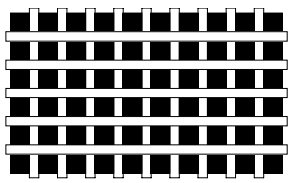

Fig. 10 Anisotropic material with high permeability in only one direction.

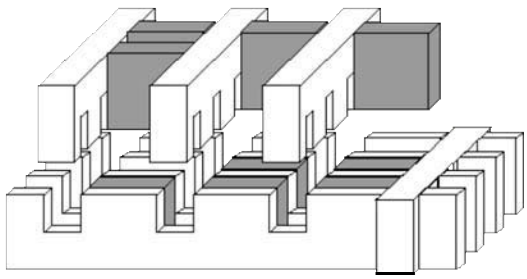

Fig. 11 One directional high μ material can be composed from magnetic material inserted in nonmagnetic separators.

Three inter-pole configurations are compared: layered material (stacked in the paper direction), single axis material (vertical) and hybrid material of these two. The first one has the same geometry as that appeared in the bottom left of Fig. 6 where the permeability in the direction normal to the paper is supposed to low, while the permeability in the horizontal direction is high. The second one has anisotropy in the paper plane and low permeability in the horizontal direction. This structure shows the less fringing field but has less uniformity in the inner gap region (see Fig. 13). The third one has the anisotropic material at only the edge. This one exhibits flat distribution at inner gap region and less fringing field.

DISCUSSIONS

Conventional magnets made of silicon steel sheets, which are usually used in AC magnets, have already this kind of layered configuration. It should be noted that the flux density at the outer most layers becomes high because of the low permeability normal to the sheet even with a Rogowskii shape (see Fig. 14). This flux concentration becomes worse for a sharp edge magnet. Because the low permeability may reduce a flux component penetrating the steel sheets, the eddy current loss may be reduced, which has been cured by cutting slits on the sheets. The high flux density, however, is supposed to cause serious saturation loss in many cases.

Although the smaller magnetic flux density caused by the smaller packing factor may restrict its applications, changing the packing factor from location to location may

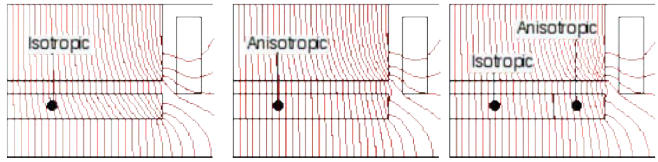

Fig. 12 Geometries to compare absolute values of the fringing field, which show the effects of the anisotropies.

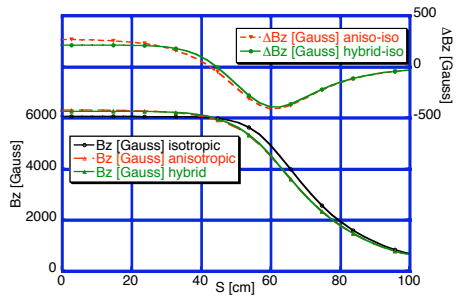

Fig. 13 Fringing fields with different anisotropies. Magnified differences from the isotropic (in the paper plane) inter-pole are also shown.

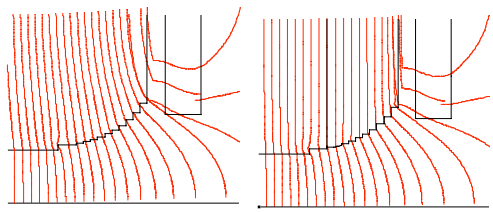

Fig. 14 Flux distributions at the magnet edges of a solid magnet (left) and a laminated magnet (right).

relieve this. Usually a high field area is localized and has less field gradient, and thus less anisotropy is required. Therefore we can use bulk iron in the high field area to improve the flux density and reduce the packing factor towards the low field region.

This anisotropic material acts as a flux guide to the easy direction although the directivity is not perfect such as an optical fiber. If we can use antimagnetic material such as superconductors, which exhibit Meissner effect, better performance will be obtained in the former layered materials. Unfortunately, there is a difficulty for a magnetic flux to penetrate superconducting material. It may be possible to get round this when the two groups of separators are insulated each other in Fig. 11.

REFERENCES

[1] Morita A, Iwashita Y, Noda A, et al. Design and measurement of a combined function magnet intended for a cancer therapy accelerator, PHYS REV SPEC TOP-AC 4 (12): art. no. 122401 Part 2 DEC 2001, Morita A, et al.: A Compact Proton Synchrotron With Combined-Function Lattice Dedicated For Cancer Therapy, Proc of the 1999 Particle Accelerator Conference, 2528-2530 (1999)

[2] A. Sato:The Prism Project at the High-Intensity Proton Machine Project, Nucl.Phys.A721:1083-1086, 2003